Application of Bayesian Inference to Characterize Risks Associated with Low Doses of Low-LET Radiation

H. SCHÖLLNBERGER and **B. R. SCOTT**
Lovelace Respiratory Research Institute
Inhalation Toxicology Laboratory
P.O. Box 5890
Albuquerque, New Mexico 87185-5890 U. S. A.
hscholln@lrri.org
bscott@lrri.org

Abstract:

Improved risk characterization for stochastic biological effects of low doses of low-LET radiation is important for protecting nuclear workers and the public from harm from radiation exposure. Here we present a Bayesian approach to characterize risks of stochastic effects from low doses of low-LET radiation. The stochastic effect considered is neoplastic transformation of cells because it relates closely to cancer induction. We have used a previously published model for neoplastic transformation called $NEOTRANS_1$. It is based on two different cellular sensitivity classes for asynchronous, exponentially growing populations (*in vitro*). One sensitivity class is the hypersensitive cell. The other is the resistant cell. $NEOTRANS_1$ includes effects of genomic damage accumulation, DNA repair during cell cycle arrest, and DNA misrepair (non-lethal repair errors). The model-associated differential equations are solved for conditions of an *in vitro* irradiation at a fixed rate. Previously published solutions apply only to high dose rates and were incorrectly assumed to apply to only high-LET radiation. Solutions provided here apply to any fixed dose rate and to both high- and low-LET radiations. Markov Chain Monte Carlo methods are used to carry out the Bayesian inference of the low-dose risk for neoplastic transformation of aneuploid C3H 10T1/2 cells for X-ray doses from 0 to 1000 mGy. We have assumed that for this low dose range only the hypersensitive fraction of the cells are affected. Our results indicate that the initial slope of the risk vs. dose relationship for neoplastic transformation is as follows: (1) directly proportional to the fraction, f_1, of cells that are hypersensitive; (2) directly proportional to the radiosensitivity of the genomic target; and (3) inversely proportional to the rate at which hypersensitive cells with radiation-induced damage are committed to undergo correct repair of genomic damage. Further, our results indicate that very fast molecular events are associated with the commitment of cells to the correct repair pathway. Results also indicate that commitment of cells to the misrepair pathway can occur with a lower frequency relative to commitment to the correct repair pathway. Our results are consistent with the view that for very low doses, dose rate is not an important variable for characterizing low-LET radiation risks so long as age-related changes in sensitivity do not occur during irradiation.

1. INTRODUCTION

The NEOTRANS$_1$ model (Fig. 1) previously published from our Institute (Scott, 1997) uses a series of genomic instability states to characterize neoplastic transformation (*in vitro*) induced by high linear-energy-transfer (LET) radiations. The term *genomic instability states* refer to any spontaneous or toxicant-induced instability in the genome, including any initial-transient instability or persistent instability that may be passed to cell progeny. In addition to a stable genome, the NEOTRANS$_1$ model also includes four types of genomic instability: (1) *Normal-minor instability* (NMI) associated with normal cell function and normal genome status; (2) *Transient-minor instability* (TMI) associated with toxicant-induced genomic damage that is fully repairable (without any significant errors); (3) *Transient-problematic instability* (TPI) associated with genomic damage that may be fully repairable but can be misrepaired; and (4) *Persistent-problematic instability* (PPI) that arises from misrepair, is persistent, and can be passed to progeny, increasing their potential for stochastic effects such as neoplastic transformation. Sensitivities of cells within asynchronous, exponentially growing populations (*in vitro*) for neoplastic transformation vary and within the model are broadly categorized as hypersensitive and resistant. A stable genome was modeled only for resistant cells.

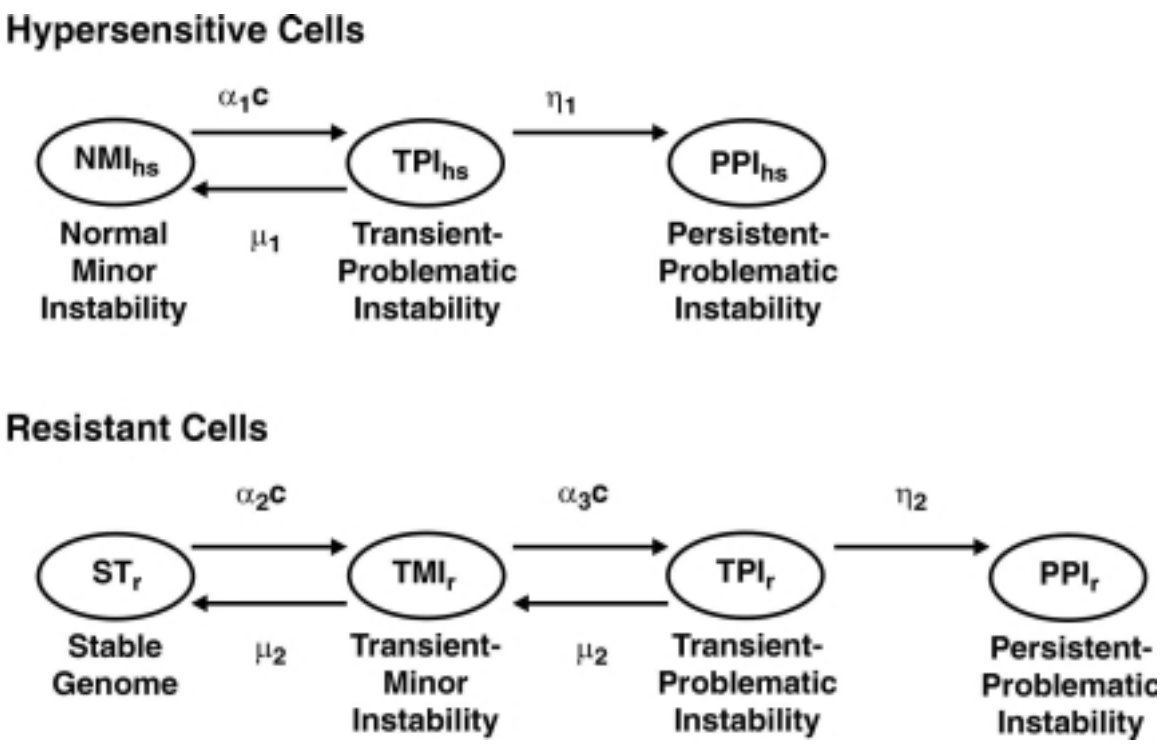

Figure 1: NEOTRANS$_1$ model for neoplastic transformation of mammalian cells. Arrows indicate pathways for instability-state transitions. Model parameters μ, η, and products αc when multiplied by Δt represent probabilities of transition between instability states when a small exposure time increment Δt is taken.

The probability that a very small dose ΔD will cause a hypersensitive cell in NMI_{hs} to enter the more unstable state TPI_{hs} during a very short time increment Δt is given by $\alpha_1 \Delta D = \alpha_1 c \Delta t$, where c is the absorbed dose rate. Hypersensitive cells in state TPI_{hs} can develop PPI genomic instability (due to misrepair) during Δt with conditional probability $\eta_1 \Delta t$. The conditional probability that a hypersensitive cell in state TPI_{hs} is repaired to state NMI_{hs} during Δt is given by $\mu_1 \Delta t$. f_1 is the fraction of hypersensitive cells with respect to neoplastic transformation. Accordingly, $1-f_1$ is the fraction of resistant cells. The probability that a very small dose ΔD will place a resistant cell in state ST_r into state TMI_r is given by $\alpha_2 \Delta D$. The corresponding conditional probability that a very small dose ΔD will place a resistant cell in state TMI_r into state TPI_r is given by $\alpha_3 \Delta D$. The conditional probability that a resistant cell in state TMI_r will be repaired to the stable state ST_r during the interval Δt is $\mu_2 \Delta t$. The corresponding conditional probability that a resistant cell in state TPI_r will be repaired to state TMI_r is also $\mu_2 \Delta t$. The conditioning is based on the absence of competing risks or processes.

Progeny of cells in state PPI_r are assumed to have a relatively high risk of undergoing spontaneous neoplastic transformation with probability Ω during a fixed follow-up time.

As with the publication of the original paper on the $NEOTRANS_1$ model (Scott, 1997), results presented here relate to transformations per surviving cell (TF/SC). Hypersensitive cells develop radiation-induced TPI via a one-step, reversible process. Mechanisms associated with this process are not known. Resistant cells develop TMI via a two-step, reversible process: the induction of TMI in stable cells and the induction of TPI in cells that have TMI. The reversible process involves the correct repair of DNA damage. However, misrepair of this damage for cells with TPI can lead to PPI that can be passed to progenitor cells rendering them susceptible to spontaneous neoplastic transformation.

$NEOTRANS_1$ was developed with the assumption that cell killing and neoplastic transformation were statistically independent effects for low-to-moderate doses of high-LET radiation (Scott, 1997). This assumption is supported by experimental data for high-LET radiation (Brenner *et al.*, 1996). Whether this is also true for low-LET radiation was unclear at that time. Thus, it was initially concluded that $NEOTRANS_1$ might apply only to high-LET radiation. Here we relax that assumption and demonstrate that $NEOTRANS_1$ can also be applied to low doses of low-LET radiation. For the dose range of interest, 0 to 1000 mGy of X-rays, we have assumed that only the hypersensitive cells are affected. However, we provide analytical solutions for both hypersensitive and resistant cells to allow for possible future application of the solutions to moderate- and high-dose data. Model parameter estimates presented here relate only to hypersensitive cells.

2. APPROACH

The differential equations associated with the model represent constant-coefficient systems of ordinary differential equations. Model equations were previously solved via the Laplace Transform method but only for very high dose rates (Scott, 1997). Here we present solutions derived using the eigenvalue method that apply to any constant dose rate. Because of the complexity of the solutions, two covariates (dose and dose rate), and data limitations, use of

standard nonlinear regression methods is problematic to obtain model parameters from experimental data. We have therefore considered a different approach.

The recent, widespread dissemination of faster computational equipment has facilitated improved statistical treatment of complex problems such as finding parameters for complicated models. An approach that has greatly benefited from these advances is Bayesian inference (Sivia, 1998; Skilling, 1989; Carlin and Louis, 1996; Miller and Inkret, 1996 a, b; Gilks *et al.*, 1997; Gamerman, 1997). Further, the rediscovery of relative simple, but extremely powerful simulation techniques has made possible the application of the Bayesian paradigm to many complex real-world problems (Gilks *et al.*, 1997; Gamerman, 1997). The techniques are collectively known as Markov Chain Monte Carlo (MCMC). We have used MCMC to derive parameter means and distributions for the $NEOTRANS_1$ model.

2.1 ***Bayesian paradigm***. For the Bayesian paradigm, there is no distinction between observable results and parameters of a model – all are considered random quantities. If "*obs*" is used to denote observed results and θ to denote model parameters and missing data, then formal Bayesian inference requires setting up a joint probability distribution $P(obs, \theta)$ over the random quantities. This joint distribution comprises two parts: a prior distribution, $P(\theta)$, and a likelihood, $P(obs|\theta)$. The vertical bar indicates that *obs* is conditional on θ. The full probability model is specified as

$$P(obs, \theta) = P(obs|\theta)P(\theta) = P(\theta|obs)P(obs) \quad (1)$$

Both $P(\theta)$ and $P(obs)$ are unconditional distributions. When new observations are available, Bayes theorem is used to obtain the distribution of the parameters $P(\theta|obs)$ given (i.e., conditional on) the observation:

$$P(\theta|obs) = P(obs|\theta)P(\theta)/\int P(obs|\theta)P(\theta)d\theta = P(obs|\theta)\, P(\theta)/P(obs) \quad (2)$$

In this study we are interested in $P(\theta|obs)$, where θ *is a vector of model parameters.* $P(\theta|obs)$ is the posterior distribution of θ given the observations, and it is the object of our Bayesian inference.

2.2 ***MCMC analyses*.** Our application of MCMC analyses to carry out Bayesian inference is based on Gibbs sampling, which is a special case of the Metropolis-Hastings algorithm (Gilks *et al.*, 1997; Gamerman, 1997). Our MCMC calculations were conducted using BUGS software (Windows version) (WinBUGS Version 1.2 User Manual, 1999) to obtain the posterior distributions for the model parameters.

Monte Carlo integration has been connected to Bayesian inference after its introduction by Kloek and van Dijk (1978). MCMC is a method of evaluating expressions of the form of equation (2) (Gilks *et al.*, 1997). The constituent parts of MCMC are Monte Carlo integration and Markov Chains.

The principle of Monte Carlo integration is reflected in the following approximation for very large N.

$$I = \int_a^b f(\theta)d\theta \approx \frac{b-a}{N}\sum_{i=1}^{N} f(\theta_i) \tag{3}$$

The right-hand side of equation (3) is evaluated numerically. Instead of choosing θ_i at regular intervals, they are chosen at random. The error is purely statistical, $\propto 1/\sqrt{N}$ independent of the dimension of the integral.

In general, drawing samples $\{\theta_i, i=1,\ldots, n\}$ independently from $\pi(.)$, the posterior distribution of the random variables (model parameters) θ, is not feasible, since $\pi(.)$ can be quite non-standard. However, the $\{\theta_i\}$ need not necessarily be independent. The $\{\theta_i\}$ can be generated by any process that draws samples throughout the support of $\pi(.)$ in the correct proportions. The support of $\pi(.)$ or any other distribution is the ensemble of x's (data) for which $\pi(x)$ is non-zero. One way of performing this sampling is through a Markov Chain having $\pi(.)$ as its designed stationary distribution. This is achieved via Markov Chain Monte Carlo (Gilks *et al.*, 1997). Suppose we generate a sequence of random variables $\{\theta_0, \theta_1, \theta_2,\ldots\}$. Each time $i\geq 0$, the next state θ_{i+1} is sampled from $f(\theta_{i+1}|\theta_i)$, which depends only on the current state of the chain θ_i. That is, given θ_i, the next state θ_{i+1} does not depend on the history of the chain $\{\theta_0, \theta_1,\ldots, \theta_{i-1}\}$. The stationary distribution of this Markov Chain is the desired posterior distribution (Gilks *et al.*, 1997).

For the prior distributions of the model parameters, α_1, μ_1, η_1, f_1, Ω and the spontaneous transformation frequency, subjective uniform distributions were used. The posterior distributions can have a very different shape than the prior distribution.

2.3 ***Data used.*** The data used to derive model parameters were taken from the literature (Miller and Hall, 1978; Miller *et al.*, 1979, 1991; Balcer-Kubiczek and Harrison, 1988) and refer to *in vitro* irradiation of C3H 10T1/2 cells by X-rays. Again, the biological endpoint under consideration was neoplastic transformation. The doses ranged from 100 mGy to 1000 mGy, and the dose rates covered the range of 320 mGy/min to 4000 mGy/min. Altogether 11 data points were pooled. They comprised four different dose rates.

3. MODEL SOLUTIONS

Two phases are considered during *in vitro* experiments for which the differential equations were defined in the irradiation phase (time regime t), denoted with subscript I, and the post-irradiation phase with the dose rate c equal to zero (Schöllnberger *et al.*, 2000). The latter is denoted with subscript II and is associated with time regime t′. Before we give the solutions of the model equations, we identify the following: $x_I(t):=NMI_{hs}(t)$, $y_I(t):=TPI_{hs}(t)$, and $z_I(t):=PPI_{hs}(t)$. $NMI_{hs}(t)$ gives the proportion of hypersensitive cells with NMI at time t, $TPI_{hs}(t)$ gives the proportion of hypersensitive cells with TMI at time t, and $PPI_{hs}(t)$ gives the proportion of hypersensitive cells with PPI at time t.

The solutions were derived in (Schöllnberger *et al.*, 2000) and are as follows:

$$x_I(t) = \frac{\mu_1 + \eta_1 + \lambda_1}{\lambda_1 - \lambda_2} e^{\lambda_1 t} + \frac{\mu_1 + \eta_1 + \lambda_2}{\lambda_2 - \lambda_1} e^{\lambda_2 t}, \tag{4}$$

$$y_I(t) = \frac{\alpha_1 c}{\lambda_1 - \lambda_2} e^{\lambda_1 t} + \frac{\alpha_1 c}{\lambda_2 - \lambda_1} e^{\lambda_2 t} \text{ and} \tag{5}$$

$$z_I(t)=1-x_I(t)-y_I(t). \tag{6}$$

with

$$\lambda_i = -\frac{\alpha_1 c + \mu_1 + \eta_1}{2} \pm \frac{1}{2}\sqrt{(\alpha_1 c)^2 + (\mu_1 + \eta_1)^2 + 2(\mu_1 - \eta_1)\alpha_1 c}, \tag{7}$$

with i=1, 2 for the results associated with equation (7).

For the post-irradiation phase we got (Schöllnberger *et al.*, 2000)

$$x_{II}(t') = x_I(t) + \frac{\mu_1}{\mu_1 + \eta_1} y_I(t)(1 - e^{\delta_2 t'}), \tag{8}$$

$$y_{II}(t') = y_I(t) e^{\delta_2 t'} \text{ and} \tag{9}$$

$$z_{II}(t')=1-x_{II}(t')-y_{II}(t') \tag{10}$$

with $x_{II}(t'):=NMI_{hs}(t')$, $y_{II}(t'):=TPI_{hs}(t')$, $z_{II}(t'):=PPI_{hs}(t')$ and $\delta_2= -(\mu_1+\eta_1)$.

For the closed form solution for the resistant cells, we define $o_I(t):=ST_r(t)$, $p_I(t):=TMI_r(t)$, $q_I(t):=TPI_r(t)$, and $r_I(t)=PPI_r(t)$. $ST_r(t)$ gives the proportion of resistant cells with stable genome at time t, $TMI_r(t)$ gives the proportion of resistant cells with TMI at time t, $TPI_r(t)$ gives the proportion of resistant cells with TPI at time t, and $PPI_r(t)$ stands for the proportion of resistant cells with PPI at time t.

We get

$$o_I(t) = \frac{\Delta_1}{\Delta}\frac{\mu_2}{\alpha_2 c + \kappa_1} e^{\kappa_1 t} + \frac{\Delta_2}{\Delta}\frac{\mu_2}{\alpha_2 c + \kappa_2} e^{\kappa_2 t} + \frac{\Delta_3}{\Delta}\frac{\mu_2}{\alpha_2 c + \kappa_3} e^{\kappa_3 t},$$

$$p_I(t) = \frac{\Delta_1}{\Delta} e^{\kappa_1 t} + \frac{\Delta_2}{\Delta} e^{\kappa_2 t} + \frac{\Delta_3}{\Delta} e^{\kappa_3 t}, \qquad (11)\text{-}(14)$$

$$q_I(t) = \frac{\Delta_1}{\Delta}\frac{\alpha_3 c}{\mu_2 + \eta_2 + \kappa_1} e^{\kappa_1 t} + \frac{\Delta_2}{\Delta}\frac{\alpha_3 c}{\mu_2 + \eta_2 + \kappa_2} e^{\kappa_2 t} + \frac{\Delta_3}{\Delta}\frac{\alpha_3 c}{\mu_2 + \eta_2 + \kappa_3} e^{\kappa_3 t} \text{ and}$$

$r_I(t)=1-o_I(t)-p_I(t)-q_I(t)$

with

$$\Delta = \begin{vmatrix} \frac{\mu_2}{\alpha_2 c + \kappa_1} & \frac{\mu_2}{\alpha_2 c + \kappa_2} & \frac{\mu_2}{\alpha_2 c + \kappa_3} \\ 1 & 1 & 1 \\ \frac{\alpha_3 c}{\mu_2 + \eta_2 + \kappa_1} & \frac{\alpha_3 c}{\mu_2 + \eta_2 + \kappa_2} & \frac{\alpha_3 c}{\mu_2 + \eta_2 + \kappa_3} \end{vmatrix},$$

$$\Delta_1 = \begin{vmatrix} 1 & \frac{\mu_2}{\alpha_2 c + \kappa_2} & \frac{\mu_2}{\alpha_2 c + \kappa_3} \\ 0 & 1 & 1 \\ 0 & \frac{\alpha_3 c}{\mu_2 + \eta_2 + \kappa_2} & \frac{\alpha_3 c}{\mu_2 + \eta_2 + \kappa_3} \end{vmatrix},$$

$$\Delta_2 = \begin{vmatrix} \frac{\mu_2}{\alpha_2 c + \kappa_1} & 1 & \frac{\mu_2}{\alpha_2 c + \kappa_3} \\ 1 & 0 & 1 \\ \frac{\alpha_3 c}{\mu_2 + \eta_2 + \kappa_1} & 0 & \frac{\alpha_3 c}{\mu_2 + \eta_2 + \kappa_3} \end{vmatrix} \text{ and}$$

$$\Delta_3 = \begin{vmatrix} \frac{\mu_2}{\alpha_2 c + \kappa_1} & \frac{\mu_2}{\alpha_2 c + \kappa_2} & 1 \\ 1 & 1 & 0 \\ \frac{\alpha_3 c}{\mu_2 + \eta_2 + \kappa_1} & \frac{\alpha_3 c}{\mu_2 + \eta_2 + \kappa_2} & 0 \end{vmatrix}.$$

Eigenvalues κ_1, κ_2, and κ_3 are evaluated as roots of the indicated cubic equation

$$\kappa^3+(\alpha_2 c+2\mu_2+\alpha_3 c+\eta_2)\kappa^2+[\mu_2^2+\eta_2(\alpha_2 c+\mu_2+\alpha_3 c)+\alpha_2 c(\mu_2+\alpha_3 c)]\kappa+\alpha_2 c\,\alpha_3 c\,\eta_2=0. \quad (15)$$

For the post-irradiation phase, we get

$$r_{II}(t')=1-o_{II}(t')-p_{II}(t')-q_{II}(t') \text{ with} \quad (16)$$

$$o_{II}(t')=\left[o_I(t)+p_I(t)+q_I(t)\frac{\mu_2}{\mu_2+\eta_2}\right]e^{\theta_1 t'}-\left[p_I(t)+q_I(t)\frac{\mu_2}{\eta_2}\right]e^{\theta_2 t'}+[q_I(t)]\frac{\mu_2^2}{(\mu_2+\eta_2)\eta_2}e^{\theta_3 t'},$$

$$p_{II}(t')=\left[p_I(t)+q_I(t)\frac{\mu_2}{\eta_2}\right]e^{\theta_2 t'}-[q_I(t)]\frac{\mu_2}{\eta_2}e^{\theta_3 t'}, \quad (17)\text{-}(19)$$

$$q_{II}(t')=[q_I(t)]e^{\theta_3 t'}$$

with $\theta_1=0$, $\theta_2=-\mu_2$, and $\theta_3=-(\mu_2+\eta_2)$.

In a cell culture that contains both hypersensitive and resistant cells, the steady-state solutions for $PPI_{hs}(t')$ must be multiplied with the fraction of hypersensitive cells, f_1. The steady-state solution is gained by forming the limit $t'\to\infty$:

$$\lim_{t'\to\infty}(s(t'))=\lim_{t'\to\infty}(f_1 z_{II}(t'))=f_1\left(1-x_I(t)-\frac{\mu_1}{\mu_1+\eta_1}y_I(t)\right), \quad (20)$$

where $z_{II}(t')$ was defined as $PPI_{hs}(t')$. $s(t')$ indicates the fraction of cells that are hypersensitive and have PPI at time t'. For $x_I(t)$ and $y_I(t)$, the solutions given in (4) and (5) must be used, and t is replaced with D/c, where D is the dose of the irradiation. Progeny of cells in state PPI are assumed to have a relatively high risk of undergoing spontaneous neoplastic transformation. The follow-up, time-dependent probability, per surviving daughter cell, of spontaneous neoplastic transformation is given by Ω. This gives the dose-response TF/SC(D) for induction of neoplastic transformation per surviving cell:

TF/SC(D)=

$$f_1\Omega\left[1-\frac{\mu_1+\eta_1+\lambda_1}{\lambda_1-\lambda_2}e^{\lambda_1 D/c}+\frac{\mu_1+\eta_1+\lambda_2}{\lambda_2-\lambda_1}e^{\lambda_2 D/c}-\frac{\mu_1}{\mu_1+\eta_1}\left(\frac{\alpha_1 c}{\lambda_1-\lambda_2}e^{\lambda_1 D/c}+\frac{\alpha_1 c}{\lambda_2-\lambda_1}e^{\lambda_2 D/c}\right)\right] \quad (21)$$

This function was used to perform Bayesian inference using a MCMC approach.

4. RESULTS

Analytical solutions for model-associated differential equations were evaluated over two time regimes: t regime (during irradiation) and t′ regime (post irradiation). Final solutions used in constructing dose-response relationships were based on steady-state solutions for the t′ regime.

Table 1 gives the doses and dose rates associated with the transformation data used in the data pool. It also gives mean predicted values for the number of transformants per survivor. These are the posterior mean values gained by MCMC. The observed data for TF/SC are given in column 4, followed by the relation of observed mean TF/SC to the corresponding posterior mean values. Column 6 gives the difference of the mean observed TF/SC and the observed mean spontaneous TF/SC divided by the corresponding dose.

Table 1: Dose rates, doses, predicted mean transformants per survivor in C3H 10T1/2 cells, observed mean transformants per 10^4 survivors, and observed mean divided by predicted mean transformants per survivor. The far right-hand column gives the difference between the observed mean TF/SC and the observed mean spontaneous TF/SC (taken from Miller *et al.*, 1995) divided by the corresponding dose. The radiation used was X-rays.

Dose rate [mGy/min]	Dose [mGy]	Predicted transformants per survivor	Observed transformants per survivor	Observed/ predicted	[TF/SC - spontan. TF/SC]/ dose
320	100	6.95E-05	6.86E-05	0.99	1.06E-07
320	300	1.03E-04	1.40E-04	1.36	2.73E-07
320	500	1.35E-04	1.52E-04	1.12	1.88E-07
320	1000	2.16E-04	1.76E-04	0.82	1.18E-07
950	300	1.03E-04	1.24E-04	1.21	2.20E-07
950	500	1.35E-04	1.33E-04	0.98	1.50E-07
950	1000	2.14E-04	1.80E-04	0.84	1.22E-07
4000	250	9.44E-05	5.10E-05	0.54*	-2.80E-08*
4000	500	1.35E-04	1.04E-04	0.77	9.20E-08
4000	1000	2.14E-04	2.46E-04	1.15	1.88E-07
780	1000	2.15E-04	2.55E-04	1.19	1.97E-07

* Results judged unreliable.

Figures 2-7 give the MCMC-generated posterior distribution for the spontaneous transformation frequency T_o, the fraction f_1 of hypersensitive cells, and the other model parameters α_1, μ_1, η_1, and Ω. Again, the parameters μ_1, η_1 govern the rate of commitment of cells to the error-free repair and misrepair pathways, respectively. The parameter Ω determines the fraction of cells with PPI that produces neoplastically transformed progeny. Results are based on 2500 MCMC iterations implemented with WinBUGS software. Results for the first 1000 iterations were discarded. Table 2 presents the mean posterior values for the model parameters, percentiles, and modes. Table 3 gives the corresponding halftime values associated with μ_1 and η_1.

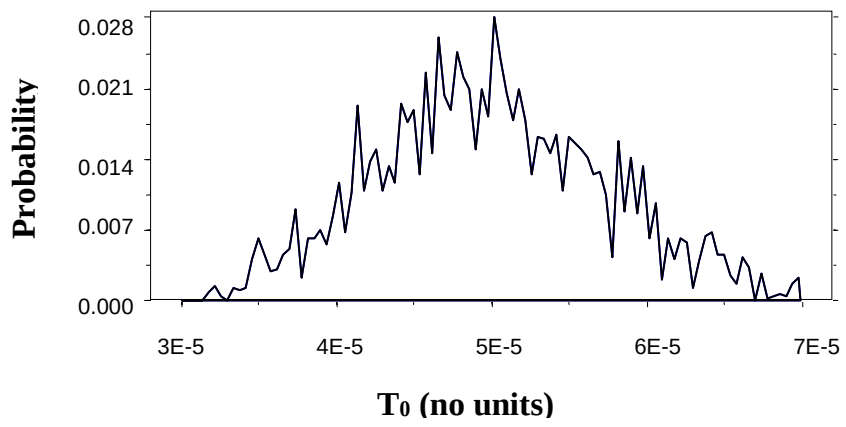

Figure 2: MCMC-generated posterior distribution for the spontaneous transformation frequency per survivor, T_0, for C3H 10T1/2 cells exposed to photon radiation. Possible values for T_0 appear on the horizontal axis and have no units. The vertical axis gives the frequency of occurrence of a given value. The mean value obtained for T_0 was $5.27 \times 10^{-5} \pm 6.63 \times 10^{-6}$. A normal prior distribution was used.

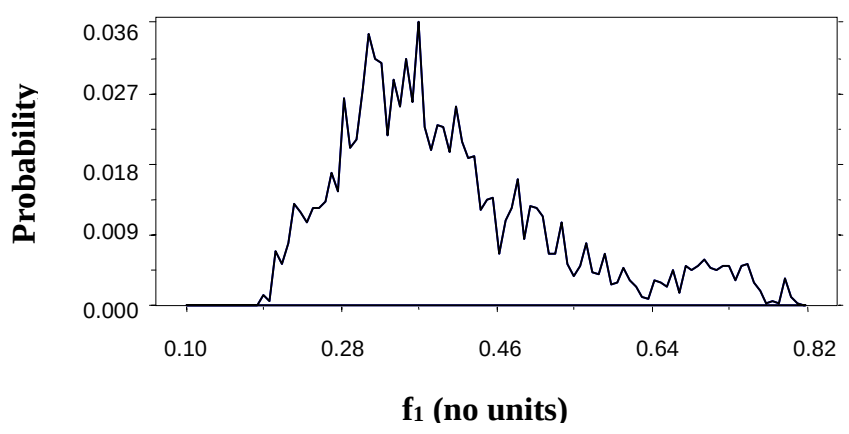

Figure 3: MCMC-generated posterior distribution for model parameter f_1. Possible values appear on the horizontal axis (negative values excluded). The vertical axis gives the frequency of occurrence of a given value. The mean value for f_1 was 0.41 ± 0.15. The large standard deviation reflects the skewed posterior distribution. A uniform prior distribution was used.

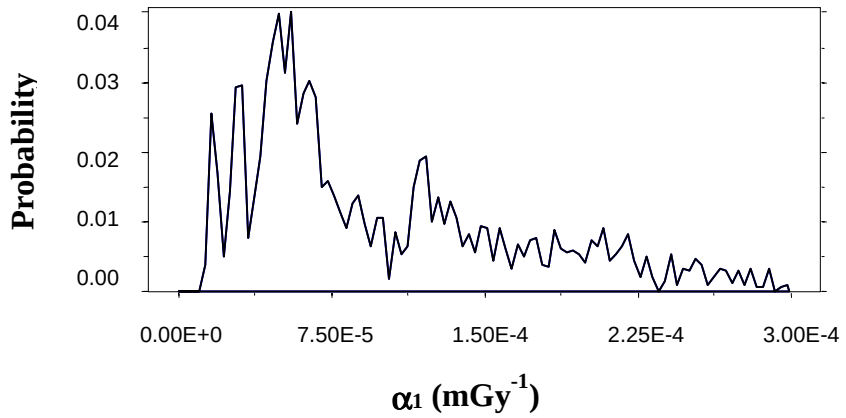

Figure 4: MCMC-generated posterior distribution for model parameter α_1 (mGy^{-1}). Possible values appear on the horizontal axis (negative values excluded). The vertical axis gives the frequency of occurrence of a given value. The mean value for α_1 was $1.02 \times 10^{-4} \pm 6.98 \times 10^{-5}$ mGy^{-1}. The large standard deviation reflects the skewed posterior distribution. A uniform prior distribution was used.

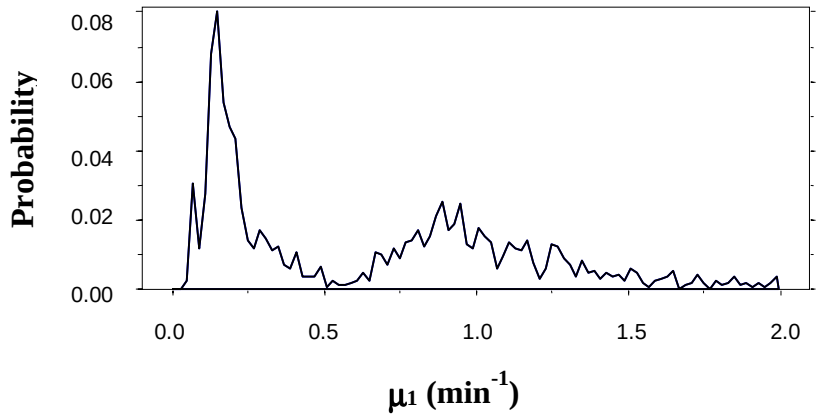

Figure 5: MCMC-generated posterior distribution for model parameter μ_1 (min^{-1}). Possible values appear on the horizontal axis (negative values excluded). The vertical axis gives the frequency of occurrence of a given value. The mean value for μ_1 was 0.65 ± 0.51 min^{-1}. Very fast molecular events related to DNA repair are suggested.

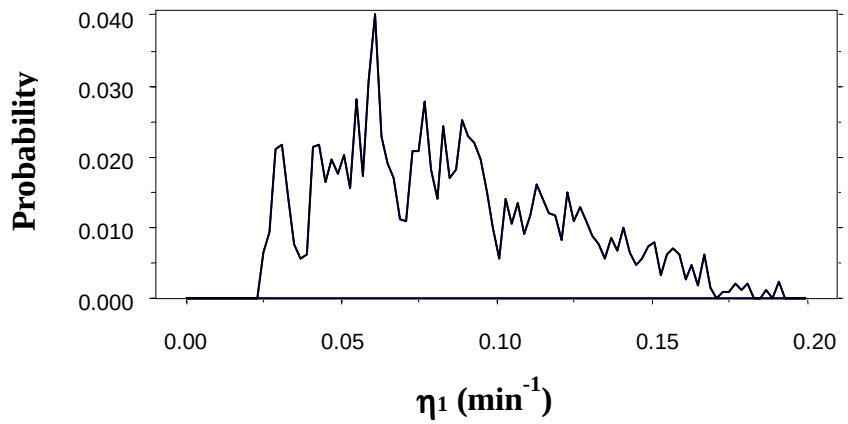

Figure 6: MCMC-generated posterior distribution for model parameter η_1 (min^{-1}). Possible values appear on the horizontal axis (negative values excluded). The vertical axis gives the frequency of occurrence of a given value. The mean value for η_1 was 0.08 ± 0.04 min^{-1}. The large standard deviation reflects the skewed posterior distribution. A uniform prior distribution was used.

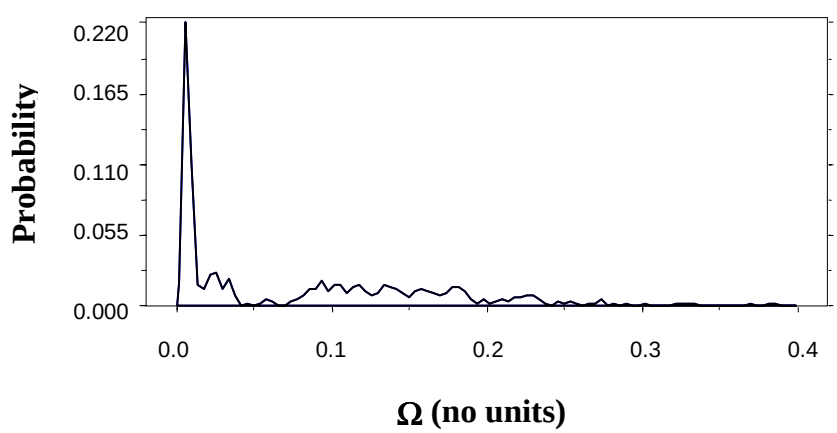

Figure 7: MCMC-generated posterior distribution for model parameter Ω. Possible values appear on the horizontal axis (negative values excluded). The vertical axis gives the frequency of occurrence of a given value. The mean value for Ω was 0.09 ± 0.10. The large standard deviation reflects the skewed posterior distribution. A uniform prior distribution was used.

Table 2: Mean, mode and percentiles of the posterior distributions for the model parameters T_0, f_1, α_1, μ_1, η_1, and Ω. Results obtained refer to *in-vitro* X-irradiation of C3H 10T1/2 cells.

Parameter	Mean	10 %	25 %	50 %	75 %	90 %	Mode
T_0	5.265E-5	4.452E-5	4.802E-5	5.223E-5	5.712E-5	6.144E-5	5.29E-05
f_1	0.4103	0.2618	0.3073	0.3702	0.4726	0.6417	0.30
α_1 [mGy^{-1}]	1.018E-4	3.018E-5	4.904E-5	7.533E-5	1.424E-4	2.094E-4	1.19E-04
μ_1 [min^{-1}]	0.6545	0.1294	0.1746	0.6386	1.007	1.321	0.14
η_1 [min^{-1}]	0.08434	0.04081	0.05643	0.07881	0.1107	0.1375	0.13
Ω	0.09437	0.005616	0.00811	0.07885	0.1543	0.224	0.11

Table 3: Percentiles for halftimes for commitment to the pathways of error-free repair and misrepair.

Percentile	Repair halftime [min]	Misrepair halftime [min]
10 %	0.52	5.03
25 %	0.69	6.25
50 %	1.07	8.79
75 %	3.97	12.28
90 %	5.36	16.98

Figures 8a-c show the calculated risk distribution for neoplastic transformation (conditional on cell survival of C3H 10T1/2 cells) for three fixed X-ray dose rates: 0.1 mGy/min, 10 mGy/min, and 1000 mGy/min. The figures show that the shapes of the risk distributions for the three different dose rates are very similar indicating no significant dose rate effect.

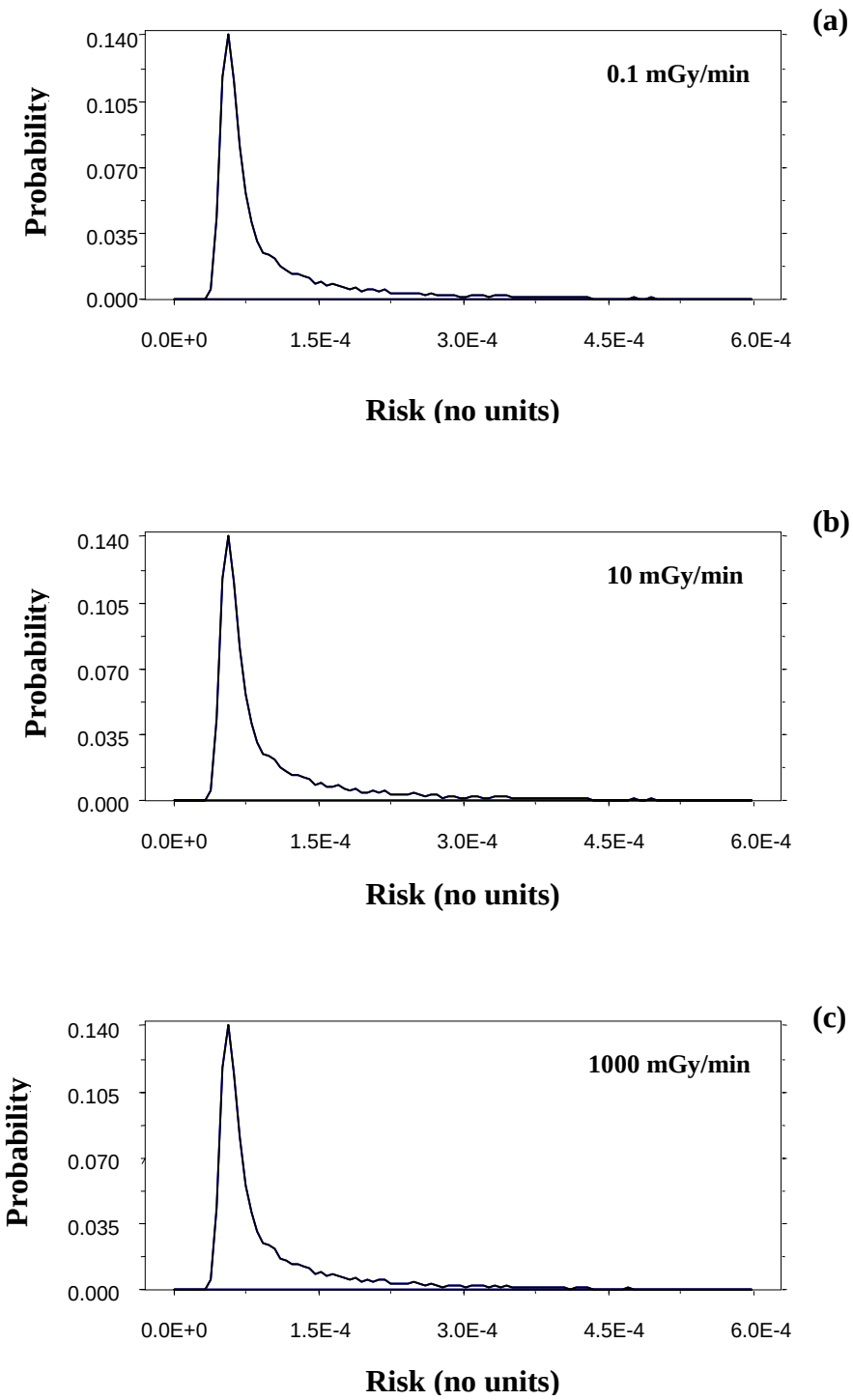

Figure 8:
a: Calculated risk distribution for X-ray-induced neoplastic transformation for a fixed dose of 100 mGy and a dose rate of 0.1 mGy/min; b: Calculated risk distribution for X-ray-induced neoplastic transformation for a fixed dose of 100 mGy and a dose rate of 10 mGy/min; c: Calculated risk distribution for X-ray-induced neoplastic transformation for a fixed dose of 100 mGy and a dose rate of 1000 mGy/min.

5. DISCUSSION

The initial slope of the dose-response curve for PPI induction is given by:

$$\left.\frac{ds(D)}{dD}\right|_{D=0} = f_1\alpha_1 \frac{\eta_1}{\mu_1 + \eta_1} . \tag{22}$$

The initial slope of the dose-response curve for neoplastic transformation is obtained by multiplying the right-hand side of equation (22) by Ω. The initial slope is independent of dose rate.

It is also visible from column 6 in Table 1 that, except for the value that refers to the largest deviation of predicted TF/SC form observed, there is essentially no dose-rate dependence of the induction of neoplastic transformation by doses lower than 1000 mGy. The correlation coefficient between the dose rates given in column 1 of Table 1 and the slopes given in column 6 is -0.23. Therefore, based on the 1% significance level for the equal-tails test of the hypothesis that the absolute value of the correlation coefficient is 0, the dose rate and slope are uncorrelated (Crow *et al.*, 1960).

Thus, based on NEOTRANS$_1$, a very small dose of radiation will induce neoplastic transformation with a probability characterized by the following:

- Is directly proportional to the fraction, f_1, of hypersensitive cells.
- Is directly proportional to the sensitivity of the genomic target in the hypersensitive cells, which is reflected by the parameter α_1.
- Is inversely proportional to the rate, μ_1, at which damaged hypersensitive cells undergo error-free repair of genomic damage.
- Is independent of dose rate.

It follows that variability in f_1 over different experimental studies using the same cell type should contribute to variability in the results obtained.

The mean posterior value of 0.65 min^{-1} for error-free repair of genomic damage in hypersensitive C3H 10T1/2 cells corresponds to a repair-halftime of 1.06 min (posterior mean). This indicates that very fast molecular events appear to be associated with this pathway. Misrepair of damage seems to occur with a somewhat lower probability: the corresponding mean posterior halftime is 8.22 min. The percentiles for α_1 and Ω indicate that the corresponding posterior distributions are highly skewed. The value of 5.26×10^{-5} for the posterior mean spontaneous transformation frequency per surviving cell is similar to the value of 4.5×10^{-5} gained in a study by Schöllnberger *et al.* (1999) where a mechanistic state-vector model was tested on the same biological endpoint. Miller *et al.* (1995) gave an observed value of 5.8×10^{-5}.

6. SUMMARY AND CONCLUSIONS

It has been shown that for this genomic instability state model of neoplastic transformation, there are closed form solutions. The analytical solutions provide greater flexibility in model applications such as data simulation on neoplastic transformation as performed in this study and facilitate gaining greater insight about model implications. Some key conclusions based on Bayesian inference carried out using MCMC analysis of data for X-ray-induced cell transformation follow:

- The initial slope for the dose-response curve for PPI induction and for the risk of neoplastic transformation for a mixed population of hypersensitive and resistant cells should be proportional to the fraction of hypersensitive cells.

- Given $f_1>0$, a small dose of radiation would be expected to induce neoplastic transformation with a probability that (1) is directly proportional to dose; (2) is directly proportional to the radiosensitivity of the genomic target in hypersensitive cells; and (3) is inversely proportional to the rate at which hypersensitive cells with radiation-induced genomic damage undergo correct repair. For doses up to 1000 mGy, the induction of neoplastic transformation does not depend on dose rate.

- Very fast molecular events appear to be associated with repair of genomic damage in hypersensitive C3H 10T1/2 cells.

- Misrepair of damage in hypersensitive C3H 10T1/2 cells appears to occur with a lower probability relative to commitment to the correct repair pathway.

- Different cells may repair/misrepair genomic damage at different rates.

ACKNOWLEDGEMENTS

The U.S. Department of Energy (DOE), Office of Science, and the DOE Environmental Management Science Program supported this research. Paula Bradley provided editorial assistance.

REFERENCES

Balcer-Kubiczek, E. K. and G. H. Harrison (1988). Effect of X-ray dose protraction and a tumor promoter on transformation induction in vitro. *Int. J. Radiat. Biol*. **54(1)**, 81-89.

Brenner, D. J., P. Hahnfeldt, S. A. Amundson and R. K. Sachs (1996). Interpretation of inverse dose-rate effects for mutagenesis by sparsely ionizing radiation. *Int. J. Radiat. Biol.* **70(4)**, 447-458.

Carlin, B. P. and R. A. Louis (1996). *Bayes and Empirical Bayes Methods for Data Analysis,* London: Chapman & Hall.

Crow, E. L., F. A. Davis and M. W. Maxfield (Eds.) (1960). *Statistics Manual,* New York: Dover Publications, Inc.

Gamerman, D. (1997). *Markov Chain Monte Carlo*, London: Chapman & Hall.

Gilks W. R., S. Richardson and D. J. Spiegelhalter (Eds.) (1997). *Markov Chain Monte Carlo in Practice,* London: Chapman & Hall.

Kloek, J. and H. K. van Dijk (1978). Bayesian estimates of equation system parameters: an application of integration by Monte Carlo. *Econometrica* **46**, 1-19.

Miller, R. C. and E. J. Hall (1978). X-ray dose fractionation and oncogenic transformations in cultured mouse embryo cells. *Nature* **272**, 58-60.

Miller, R. C., E. J. Hall and H. H. Rossi (1979). Oncogenic transformation of mammalian cells in vitro with split doses of x-rays. *Proc. Natl. Acad. Sci. USA* **76(11)**, 5755-5758.

Miller R. C., C. R. Geard, S. A. Marino, M. Richards and G. Randers-Pehrson (1991). Oncogenic transformation following sequential irradiations with monoenergetic neutrons and X rays. *Radiat. Res*. **125**, 338-342.

Miller, R. C., S. A. Marino, D. R. Brenner, S. G. Martin, M. Richards, G. Randers-Pehrson and E. J. Hall (1995). The biological effectiveness of radon-progeny alpha particles. II. Oncogenic transformation as a function of linear energy transfer. *Radiat. Res*. **142**, 54-60.

Miller, G. and W. C. Inkret (1996a). Bayesian maximum posterior probability method for interpreting plutonium urinalysis data. *Maximum Entropy and Bayesian Methods*, Boston: Kluwer Academic Publishers, pp. 367-373.

Miller, G. and W. C. Inkret (1996b). Bayesian maximum posterior probability method for interpreting plutonium urinalysis data. *Radiat. Prot. Dosim.* **63**, 189-196.

Schöllnberger, H., M. Kotecki, D. J. Crawford-Brown, W. Hofmann and P. M. Eckl (1999). Adaptive response and dose-response plateaus for initiation in a state-vector model of carcinogenesis. *Int. J. Radiat. Biol*. **75(3)**, 351-364.

Schöllnberger, H., B. R. Scott, M. Stafford and S. Osovets (2000). Analytical solutions for a mechanistic model for radiation-induced neoplastic transformation. http://www.radiation-scott.org/neotrans1.pdf.

Scott, B. R. (1997). A mechanistic model for neoplastic transformation of cells by high LET radiation and its implications for low dose, low dose rate, risk assessment. *Radiat. Prot. Dosim*. **72(2)**, 105-117.

Sivia, D. S. (1998). *Data Analysis, A Bayesian Tutorial*, New York: Oxford University Press, Inc.

Skilling, J. (Ed.) (1989). *Maximum Entropy and Bayesian Methods*, Dordrecht: Kluwer Academic Publishers.

Spiegelhalter, D. J., A. Thomas and N. G. Best (Eds.) (1999). *WinBUGS Version 1.2 User Manual*, MRC Biostatistics Unit, Cambridge, GB.